Journal of Geochemical Exploration 185 (2018) 130–138

Contents lists available at ScienceDirect

Journal of Geochemical Exploration

journal homepage: www.elsevier.com/locate/gexplo

K-feldspar composition as an exploration tool for pegmatite-type rare metal deposits in Altay, NW China

Yong Tang[a], Hong Wang[a,b], Hui Zhang[a,*], Zheng-Hang Lv[a]

[a] Key Laboratory for High Temperature and High Pressure Study of the Earth's Interior, Institute of Geochemistry, Chinese Academy of Sciences, Guiyang 550081, PR China.

[b] University of Chinese Academy of Sciences, Beijing 100049, PR China

ARTICLE INFO

Keywords:
K-feldspar
Trace elements
P_2O_5
Pegmatite
Altay

ABSTRACT

Trace elements of potassium feldspar (Kfs) from pegmatite veins in the Keketuohai pegmatite district were determined in situ by LA-ICP-MS. As the K/Rb ratio decreases, the contents of compatible Ba and Sr decrease, while the contents of incompatible Li, Cs and Ga increase. The K/Rb ratios and above mentioned trace element contents of Kfs from the Be-Nb-Ta mineralized pegmatite veins match those of Kfs from barren pegmatite veins. In contrast, the mineralized pegmatites are characterized by having K-feldspars with high phosphorus contents, mostly above 0.1 wt% P_2O_5, which is the boundary separating mineralized pegmatites and barren pegmatites. The high P_2O_5 content in Kfs indicates high concentration of this element in the melt from which these pegmatites crystallized. The P_2O_5 content in K-feldspar can be used as an exploration tool for LCT type Be-Nb-Ta deposit.

1. Introduction

Granitic rare-element pegmatites host several economic commodities, such as the lithium hosted in spodumene and petalite, the rubidium contained in lepidolite and K-feldspars, cesium in pollucite, the beryllium in beryl, and the niobium and tantalum hosted in Nb-Ta-oxide minerals, ceramic grade feldspar, and industrial mica (e.g., Linnen et al., 2012; London, 2008 and references therein). More than 100,000 pegmatite veins have been identified in Altay, in northwest China and these veins are divided into 38 pegmatite districts. Approximate 1000 pegmatite veins are mineralized with Be, Li, Ta and Nb. The Altay pegmatite province has been the principle source of rare element and industrial mica in China (Zou and Li, 2006). The most economically important is the Keketuohai No.3 pegmatite vein, which was discovered in 1935 and mined since 1950 by a Chinses-Former Soviet Union mining company (Zou and Li, 2006). A total of 528,419 tons of spodumene, 10,592 tons of beryl, 567 tons of columbium-tantalum minerals, and 86 tons of pollucite were mined from this pegmatite vein between 1950 and 1999. After nearly half a century of mining, most of the rare-metal deposits in Altay have been either mined out or closed. Current demand for the rare metals of Li, Be, Nb and Ta in China has encouraged exploration of new deposits in this region.

Identification of pegmatite veins in Chinese Altay is relative easy because they are well exposed. Once a pegmatite dike has been located, the next step is to assess its mineralization potential. However, the study of zoned pegmatite vein by classical petrologic methods such as whole-rock chemical analysis is hampered by the coarse grain size of minerals and by the heterogeneity of large sections of the pegmatite. As stressed by previous studies, trace element contents of some minerals, such as feldspar, mica and accessory minerals (including tourmaline and garnet), are very useful geochemical indicators to assess not only the differentiation degree but also the potential for rare element mineralization in pegmatites (Alfonso et al., 2003; Černý et al., 1985; Neiva, 1995; Oyarzábal et al., 2009; Shearer et al., 1985; Smeds, 1992; Trueman and Černý, 1982).

In this paper, we present a geochemical study of K-feldspars from representative bodies of pegmatites in the Keketuohai pegmatite district in the Altay pegmatite province. Our aim is to assess the rare-element mineralization potential of pegmatites from the amounts of trace elements in K-feldspars and to find a reliable prospecting criterion.

2. Geologic background

2.1. Regional geology

The Chinese Altay orogen is situated between the south Siberian craton to the north and the Junggar block to the south. Northwest trending faults are widely developed in the Chinese Altay orogen, such

* Corresponding author.
E-mail addresses: tangyong@vip.gyig.ac.cn (Y. Tang), zhanghui@vip.gyig.ac.cn (H. Zhang).

https://doi.org/10.1016/j.gexplo.2017.11.015
Received 7 April 2017; Received in revised form 17 October 2017; Accepted 21 November 2017
Available online 24 November 2017
0375-6742/

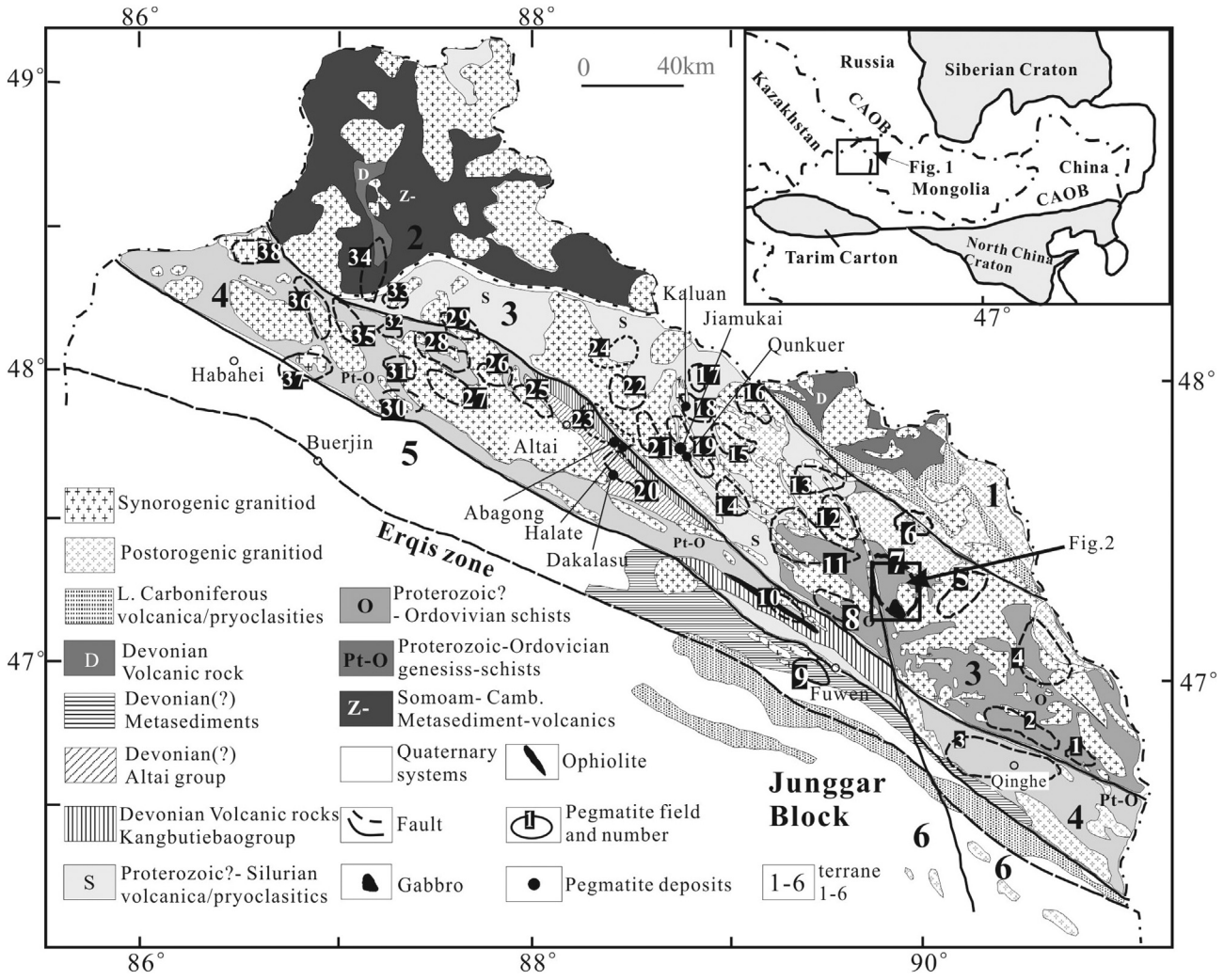

Fig. 1. The location and regional geological map of the Chinese Altay orogen. Dashed circles with number indicate pegmatite field of concentrated pegmatite veins. CAOB = Central Asian Orogenic Belt.

as the Hongshanzui fault, the Abagong fault, the Tesibahan fault, and the Irqis fault. Based on the context of stratigraphic, metamorphic, deformation, and magmatic features, five or six terranes or tectonic units have been distinguished in the Chinese Altay orogen and are separated by these NW-trending faults (Fig. 1) (Windley et al., 2002).

Terrane 1 forms the northern part of the Altay. It consists largely of Devonian to Early Carboniferous metavolcanic (andesite and dacite) and metasedimentary rocks. Terranes 2 and 3 form the central part of Altay and are an important part of the Altay microcontinent. Terrane 2 consists of Neoproterozoic (Sinian) to Middle Ordovician low-grade metamorphosed sedimentary and volcanic rocks (Habahe Group), with minor Early Devonian sedimentary and volcanic rocks. Terrane 3 is composed of amphibolite- and greenschist-facies metasediments and metavolcanics. Terranes 4 and 5 are located in southern Altay, in which Terrane 4 consists predominately of Silurian to Devonian low-grade metamorphosed arc-type volcanic rocks and Terrane 5 is mainly composed of Devonian fossiliferous successions, which are, in turn, overlain by late Carboniferous formations. Locally, gneisses and schists also occur. Terrane 6 is made entirely from Devonian island arc rocks with small amounts of Ordovician limestones and some Carboniferous island-arc volcanics. This terrane belongs to the Junggar block and is separated from the Altay orogen (Terrane 5) by the Irqis fault, one of the largest transcurrent faults in Central Asia (Sengör et al., 1993).

Approximately 200 granitoid plutons occupy at least 40% of the Chinese Altay (Zou et al., 1989), indicating that magmatism played an important role in the development of the Chinese Altay. The emplacement of these granites is episodic from the early Cambrian to the Permian, and 80% of them have ages between 450 Ma and 380 Ma with a peak ca. 400 Ma (Cai et al., 2011a, 2011b; Tong et al., 2014; Wang et al., 2006; Wang et al., 2010; Yuan et al., 2007b). The granitic intrusions that were emplaced earlier than 300 Ma are metaluminous to peraluminous in composition. Geochemical studies suggest that the metaluminous and peraluminous granites were derived from a mixture of continental sources and mantle-derived components, although the relative proportions of the mixture remains controversial (Cai et al., 2011a; Yu et al., 2017; Zhang et al., 2017). A-type granites with emplacement ages younger than 300 Ma are dominantly alkali feldspar granites and were interpreted as post-tectonic granitoids (Tong et al., 2014).

2.2. The Keketuohai granitic pegmatite district

The Keketuohai granitic pegmatite district (No.7 pegmatite district in Fig. 1) is located in the eastern part of Terrane 3. This district occurs along the fold axis of the Qinghe-Halong anticline. The Keketuohai region is mainly composed of Quaternary sediments and Ordovician schist (namely, Habahe Group), several mafic-ultra mafic complexes, abundant granitoid intrusions, and pegmatite veins (Fig. 2). Quaternary sediments are distributed along the Irqis River. The Habahe Group is composed of biotite-plagioclase-quartz schist with staurolite, biotite-

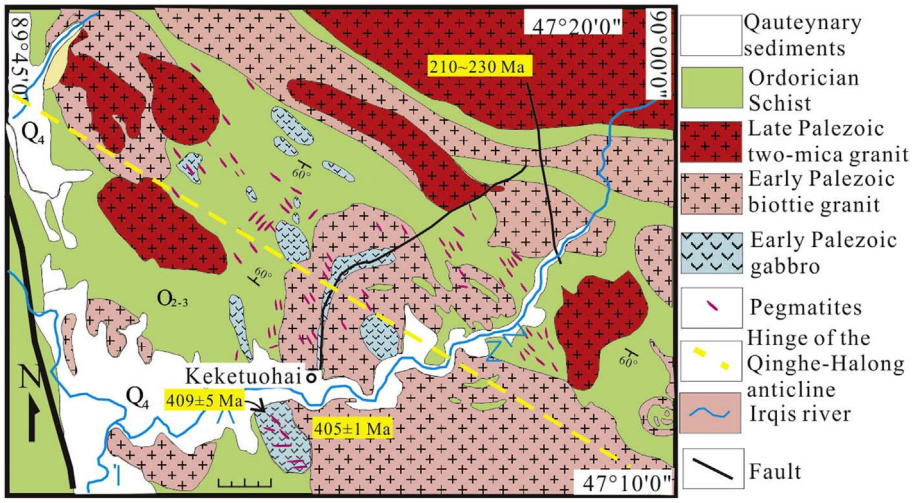

Fig. 2. Detailed geological map of Keketuohai pegmatite district, the size of pegmatites is amplified.

quartz schist with andalusit, and quartz-biotite schist, metamorphosed to greenschist and amphibolite facies. The ages of the detrital zircons constrain the deposition time of the Habahe Group to be Mid-Ordovician to Early Devonian (Yuan et al., 2007a). The ultramafic-mafic complex in the Keketuohai region shows a concentrically zoned structure that has dunite in the core, surrounded by olivine gabbro, hornblende gabbro and pyroxene diorite. LA-ICP-MS zircon U-Pb dating yielded an age of 408–409 Ma for this intrusion (Cai et al., 2012; Wang et al., 2006). The granitoid intrusions, which are composed of gneissic biotite granite, are widely distributed in this district and have an age between 409 and 416 Ma (Wang et al., 2006). The Alaer granite batholith located in the northeastern part of the district has an age of 210–232 Ma (Zhang et al., 2015).

> 3000 pegmatite veins hosted by biotite granites, schist and metagabbro, occur in the Keketuohai district. These pegmatites belong to the LCT family based on the classification scheme of (Černý and Ercit, 2005) with mineralogical characteristics ranging from barren to Be-, Ta-, and Nb-enriched types. The pegmatites intruded the biotite-granite, metagabbro plutons and the schists. The shape of the pegmatites is predominantly lenticular (Fig. 3a-3d). The vast majority of pegmatites strike WNW. Based on dip angles, the Keketuohai pegmatite veins can be divided into two groups: moderately dipping sills (dips of 0–55°) and steeply dipping dykes (dips of 70–90°). From the north to south, the dip direction of pegmatites changes from the WSW to the ENE. The thickness of the moderately dipping sills ranges from 0.5 to 40 m and the steeply dipping dykes is 0.1–1 m. The formation of the pegmatite dykes, and sills are closely related to the structures in the Keketuohai district. The WNW trending foliations and joints in the plutons, and the WNW trending schistosity in the shist are simultaneously generated by the folding of the Qinghe-Halong anticline. Pegmatite melt, which intruded into these low-pressure positions, formed different types of pegmatites. The axial plane of the Qinghe-Halong anticline is the boundary of the dip directions. Few pegmatite laccoliths are also found, such as No.3 pegmatite, and this pegmatite is controlled by faults (Tian et al., 2016).

Usually, the pegmatites have a sharp contact with the host rocks, with a narrow zone of wall-rock alteration (Fig. 3a–d). The contact aureoles in the metagabbroic wall rock mainly manifest as tourmalinization, chloritization and biotitization. The contact aureoles in the biotite-granite wall rock are characterized by silicification and greisenization. The contact aureoles in the schist are typically greisenized.

The mineralogy of the pegmatites includes quartz, K-feldspar, albite, spodumene, various micas (lepidolite, muscovite and minor cookeite), columbite-group minerals, apatite, tourmaline, beryl, lithiophilite, and spessartite. A wide variety of distinct mineralogical zonations occur in various pegmatite veins of this region. Generally, the barren pegmatites are weakly zoned, and three commonly internal textural zones can be recognized: the K-feldspar-quartz graphic zone, the blocky K-feldspar zone and the muscovite-quartz zone. Mineralized pegmatites are characterized by containing rare element minerals, such as beryl, columbite-tantalite group minerals and spodumene. The mineralized pegmatites contain a total of thousands of tons of beryl, hundreds of tons of spodumene, and tens of tons of columbite-tantalite group minerals. The mineralized pegmatites are well zoned, including in addition to those mentioned above, the saccharoidal albite zone, quartz-cleavelandite-spodumene and lepidolite-lamellar albite zone. The Keketuohai No.3 pegmatite vein is the most evolved of the well-zoned pegmatites in the Chinese Altay pegmatite province (Tang and Zhang, 2015; Wang et al., 2007; Zhang et al., 2008; Zhou et al., 2015; Zou et al., 1986). It is composed of two major parts: a gently dipping 'plate' and a steeply dipping 'cupola' protruding upwards from the plate. The cupola-shaped part is c. 250 m (in length) × 150 m (in width) × 250 m (in depth), showing a typical concentric ring structure of 9 textural zones from the rim to its core: I. Graphic zone; II. Saccharoidal albite zone; III. Blocky microcline zone; IV. Muscovite-quartz zone; V. Cleavelandite-spodumene zone; VI. Quartz-spodumene zone; VII. Thinly bladed albite-muscovite zone; VIII. Lepidolite-thinly bladed albite zone; IX. Blocky and microcline core.

3. Sample description and analytical method

The pegmatite samples were collected from quarries or/and natural exposures. The locations of these pegmatites are given in Appendix A. To ensure the comparability of the samples, samples of K-feldspar were selected from a blocky K-feldspar zone of each pegmatite vein. The detailed description of pegmatite veins, which K-feldspar samples come from, is given in Appendix B. Five samples were obtained from the same pegmatite vein, and chips of K-feldspars were mounted and made into polished thin sections for observation and analysis. In general, all of the specimens were gray white in color (Fig. 3e and f). All the K-feldspar samples exhibited perthitic texture and microcline have chessboard twinned. Fig. 4 shows some typical features of perthitic textures and twin patterns observed in the specimens studied. The high-quality trace element data of the selected-area of K-feldspar were obtained using LA-ICPMS. Pristine areas were selected that avoided large and small albite veins, turbid areas with strong alteration, inclusions of other minerals, and cracks.

Major and trace element concentrations in K-feldspars were determined using an ELAN DRC-e ICP-MS coupled with a GeoLasPro 193 nm laser system at the State Key Laboratory of Ore Deposit Geochemistry, Institute of Geochemistry, Chinese Academy of Sciences. The operating conditions for the laser ablation system, ICP-MS and data

Fig. 3. a–c) examples of pegmatite veins with variable dipping in the Keketuohai pegmatite district, a: pegmatite (KKP080, located in Xiaoshuidianzhan) has an approximately horizontal dips, b: pegmatite (KKP009, located in Xiaofusite) has a moderate dips, c: pegmatite (KKP098, located in Chaihuogou) has near vertical dips; d) one pegmatite (KKP070, located in Telanbai), intrude into biotite granite with a clear contact; e–f) typical blocky K-feldspar from pegmatite veins in Keketuohai pegmatite district.

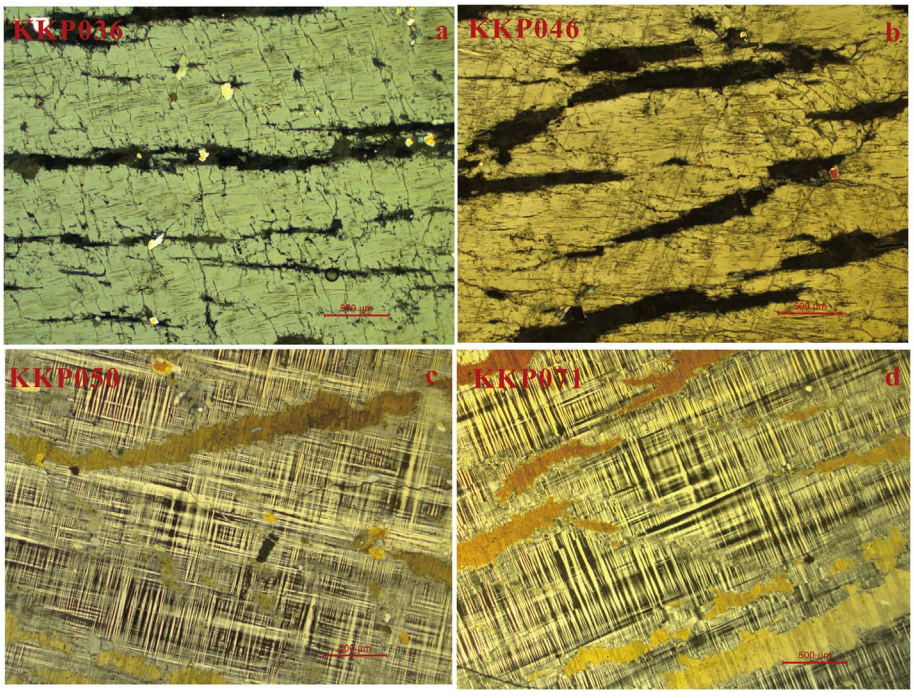

Fig. 4. Perthitic texture and twin patterns of selected K-feldspar samples from pegmatite vein in Keketuohai district. a) and b): K-feldspars from pegamite veins (KKP036 and KK046) exhibit perthitic texture; c and d): K-feldspars from pegmatite (KK050 and KK071) with perthitic texture showing chessboard twin parttern.

reduction are the same as those described by description by Liu et al. (2008). Isotopes of 52 elements were analyzed in peak jumping mode using a 44 μm spot size, a repetition rate of 10 Hz and a laser energy density of approximately 10 J/cm^2. Each analysis incorporated a background acquisition of approximately 20–30 s (gas blank) followed by 40 s of data acquisition from the sample. Helium was used as the carrier gas for the ablated material and was mixed with argon before entering the ICP-MS. Element contents were calibrated against multiple-reference materials: USGS synthetic basalt glass GSE-1G, USGS basalt glass of BCR-2G, BIR-1G, and BHVO-2G, (http://crustal.usgs.gov/geochemical_reference_standards/microanalytical_RM.html) (Liu et al., 2008). Based on the normalization of the sum of all the oxides to 100 wt% for a given anhydrous silicate mineral, the following equations by Liu et al. (2008) were used to conduct the quantitative analysis by LA-ICP-MS:

$$\begin{cases} C_{sam}^{i} = \dfrac{100 \times cps_{sam}^{i} \times l^{i}}{\sum_{k=1}^{N}(cps_{sam}^{k} \times l^{k})} \\ l^{i} = \sum_{j=1}^{n}\left(\dfrac{C_{rmj}^{i}}{cps_{rmj}^{i}} \bullet \dfrac{C_{rmj}^{i}}{\sum_{j=1}^{n} C_{rmj}^{i}}\right) \end{cases}$$

where N is the number of elements that can be determined by LA-ICPMS, n is the number of reference materials used as external standards, $C_{sam}{}^{i}$ and $C_{rmj}{}^{i}$ are the concentrations of element i in the sample and the reference material j, respectively, and $cps_{sam}{}^{i}$ ($cps_{sam}{}^{k}$) and $cps_{rmj}{}^{i}$ are the net count rates (analyte signal minus background) of element i (k) in the sample and the reference material j, respectively. When multiple reference materials were used for calibration, l value could be calculated using regression statistics of the used reference materials.

Off-line selection and integration of the background and analytic signals, the time-drift correction and quantitative calibration were performed using ICPMSDataCal (Liu et al., 2008). The limits of detection were 4.90 ppm of Li, 0.50 ppm of Rb, 0.07 ppm of Cs, 0.05 ppm of Sr, 0.05 ppm for Ba, 0.10 ppm of Pb, 0.30 ppmof Ga, and 0.04 wt% of P_2O_5.

4. Results

The analytical results are listed in Appendix C. The orthoclase (Or) component of the bulk K-feldspar ranges between Or_{80} and Or_{97} with an average value of Or_{93}. Considering the pegmatite discrimination of Fe-P content in K-feldspars, the studied pegmatites belong to the group III pegmatite according to Sánchez-Muñoz et al. (2017), as shown in Fig. 6a.

LA-ICPMS analyses indicate that Rb is the most abundant minor element in K-feldspar. The concentration of Rb varies from 460 to 4700 ppm. The K/Rb ratio ranges from 26 to 260.

Generally, the Li content of K-feldspar samples ranges from below the detection limit to 110 ppm, with most values not exceeding 50 ppm. However, there is one exception: a K-feldspar sample from a spodumene-bearing pegmatite in Kujierte pegmatite has > 100 ppm Li. As seen in Fig. 5a, though somewhat erratic, the amount of Li generally increases as the K/Rb ratio decreases.

The Cs content varies from 5 to 600 ppm, with most values lying between 5 and 200 ppm. In Fig. 5b, the Cs content is plotted against the K/Rb ratio for all K-feldspar samples. There is an overall negative correlation between Cs and K/Rb. The lines discriminating K-feldspar of barren pegmatites from those with Be, Li-Be, and Li-Cs-Be-Ta mineralization are from Trueman and Černý (1982). These lines are taken from a study of the Winnipeg River pegmatite district, southeastern Manitoba (Canada).

K-feldspars contain 0.1 to 514 ppm Ba, and 0.1 to 142 ppm Sr. The compatible elements strontium and barium exhibit a meaningful variation related to the evolution. Both Ba and Sr correlate positively with K/Rb ratio (Fig. 5c and 4d).

The amount of gallium varies from 7 to 38 ppm and exhibit an negative correlation with K/Rb ratio (Fig. 5e).

The P_2O_5 contents of the K-feldspars range from below the detection limit to 0.44 wt%. The P_2O_5 contents of the K-feldspars from mineralized pegmatites vary from 0.04 to 0.44 wt%. Only 36 of 157 studied samples, accounting for approximately 23% of the total spots, show < 0.10 wt% P_2O_5. The remaining samples contain > 0.10 wt% P_2O_5. The P_2O_5 contents of the K-feldspars from barren pegmatites range from below the detection limit to 0.16 wt% P_2O_5, in which 69 of 311 samples, accounting for 22% of the analytical samples, are below the detection limit (< 0.04 wt%) and 206 samples (approximately 66%) show 0.04–0.10 wt% and 36 samples (~12%) show > 0.10 wt% P_2O_5. Therefore, 88% of the analytical samples contain < 0.1 wt% P_2O_5. In the K/Rb-P_2O_5 plot (Fig. 5f), P_2O_5 does not exhibit any meaningful variation as K/Rb increases, but 0.1 wt% P_2O_5 adequately separates the Be-Nb-Ta mineralized pegmatites from the barren pegmatites.

5. Discussion

The trace elements in K-feldspar are very useful geochemical indicators to assess not only the differentiation degree but also the potential for rare-metal mineralization in pegmatite. The most key trace elements in K-feldspar are Li, Rb, Cs, Sr, Ba, and P (as P_2O_5). Gordiyenko (1971) proposed that feldspars with high concentration of Li, Rb, and Cs could be used to prospect for rare-metal pegmatites. Trueman and Černý (1982) utilized K/Rb ratios and Cs concentration of K-feldspars to determine pegmatite type, assess economic potential, and evaluate the genetic relationship between individual pegmatites. They recommended that the internal evolution of a single pegmatite and the petro-genetic relationships between pegmatite fields could be addressed from the trace elements in the K-feldspar. Smeds (1992) found that elevated contents of Li (> 80–100 ppm) in K-feldspar are a more reliable indicator for spodumene-bearing pegmatites than contents of Li in muscovite.

Much like previously reported pegmatites, the contents of Li, Cs, and Ga in K-feldspar from this study increasing with decreasing K/Rb ratio. The linear trend shown in a double logarithmic diagram of K/Rb vs. Li, Cs and Ga (Fig. 5) indicates that fractional crystallization may be the only process involved in the chemical trend. These ratios commonly suggest the degree of fractionation of commercially interesting lithophile elements such as Li, Be, Nb, Ta, and they indicate the qualitative geochemical potential of the examined pegmatites to carry valuable mineralization at a certain fractionation level. However, it is necessary to exercise caution when using the K/Rb or K/Cs ratio as a criterion for rare-element mineral exploration, because the overall range of these ratios among and even within individual pegmatite types is large and variable. Černý et al. (1984) found that the K/Rb ratio changes from 390 to 95, over a distance of only 1.5 m from border zone to core-margin, in a relatively primitive pegmatite of the beryl-columbite type.

The structure of alkali feldspars consists of three-dimensionally linked SiO_4 and AlO_4 tetrahedral units. There are four spectroscopically non-equivalent tetrahedrally coordinated (T) sites in each ring of tetrahedral, which are arranged in double crankshaft chains (Taylor, 1965). The alkali A^+ and alkaline earth A^{2+} elements are located on the M sites inside the irregular cavity formed by the framework of tetrahedra. The atoms at the T sites can be replaced by 5 +, and 4 + and 3 + cations, such as P^{5+}, Ge^{4+}, Ga^{3+}, and Fe^{3+}. Similarly, K and Na in the cavity M sites can be occupied by 1 +, 2 + and 3 + cations, such as Li^+, Rb^+, Cs^+, Sr^+, Ba^{2+} and REE^+.

There are three species of K-feldspar: sanidine, orthoclase and microcline. Starting from the high-temperature crystallization of a pegmatite-forming melt, the first-formed alkali feldspar at the magmatic stage is sandine, a disorder solid-solution with a composition close to (Na, K)$AlSi_3O_8$, which incorporates other cations in the framework T and cavity M sites as chemical impurities. However, as temperature

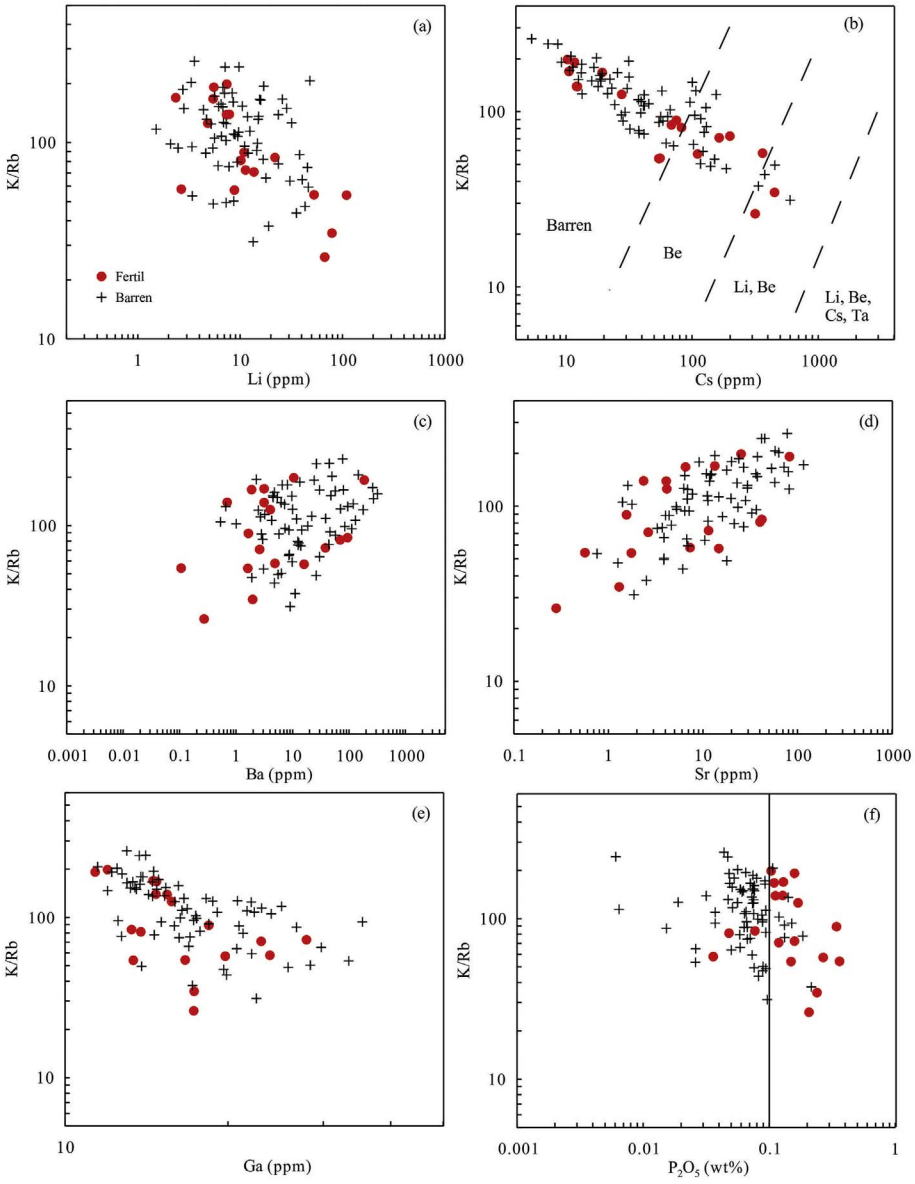

Fig. 5. Li, Cs, Ba, Sr, Ga and P_2O_5 contents against K/Rb values for K-feldspars from Keketuohai pegmatite district. a) K/Rb vs. Li; b) K/Rb vs.Cs, The discrimination lines (dash lines) from Trueman and Černý (1982) separating barren pegmatite from Be, Li-Be, and Li-Be-Cs-Ta mineralized pegmatite; c) K/Rb vs. Ba; d); K/Rb vs. Sr; e) K/Rb vs.Ga and f) K/Rb vs. P_2O_5.

decrease after emplacement, the feldspar system evolves to more equilibrated configurations by subsolidus transformations (Si-Al ordering, transformation twinning, and recrystallization twinning, as described in Sánchez-Muñoz et al., 2012). The transformations of affecting the sanidine to produce orthoclase or microline (or both) and albite involve a drastic variability in the concentrations of some elements. Consequently, the concentration of minor and trace elements in K-feldspar mainly depend on the composition of the original melts and the relevant partition coefficients, and the extent of recrystallization.

Recently, Sánchez-Muñoz et al. (2012) found that the trace elements at M site cannot be used to discriminate the different types of pegmatite, because these elements are easily released from the mineral structure during the subsolidus transformation process. However, elements like P at T site are much more firmly held in the structure. Therefore, using the elements at T sites is possible to discriminate different types of pegmatites (Fig. 6) (Sánchez-Muñoz et al., 2017). Based on major petrological features (such as the abundance of quartz, feldspars, micas and phosphate), Sánchez-Muñoz et al. (2017) classified pegmatite into four group and proposed that the Fe and P contents in K-feldspar can be used to effectively discriminate among the four groups of pegmtites. As shown in Fig. 6, pegmatites in Keketuohai district are plotted in the group III field. According to Sánchez-Muñoz et al. (2017), the pegmatites of group III consists of relatively flux-rich, silica-rich and P-poor pegmatites with quartz, subsolvus feldspar and muscovite as the major primary minerals. As mentioned above, the major minerals of the pegmatites in Keketuohai are quartz, feldspars, and mica. The mineral feature of pegmatites in Keketuohai district meets the classification criteria of Sánchez-Muñoz et al. (2017). Furthermore, Pegmatites of group III always are formed during late- to post-orogenic relaxation in an extensional environment (Sánchez-Muñoz et al., 2017). Pegmatites in Keketuohai district were mainly emplaced at Triassic (Liu et al., 2014; Ren et al., 2011; Wang et al., 2007; Zhang et al., 2016; Zhou et al., 2015). The formation of these pegmtites is usually later than the formations of A-type in Keketuohai district, which were interpreted as the product of late- or post- Chinese Altay orogen (Tong et al., 2014). In a word, the geotectonic features of pegmatites in Keketuohai district are similar to the features of pegmatites of group III proposed by Sánchez-Muñoz et al. (2017).

Phosphorus can substitute into natural and synthetic alkali feldspars by the exchange $AlPSi_{-2}$ (Simpson, 1977; London et al., 1990), but ^{31}P magic-angle spinning nuclear magnetic resonance implies that the structure mechanism of phosphorus in K-feldspar is complex and varies

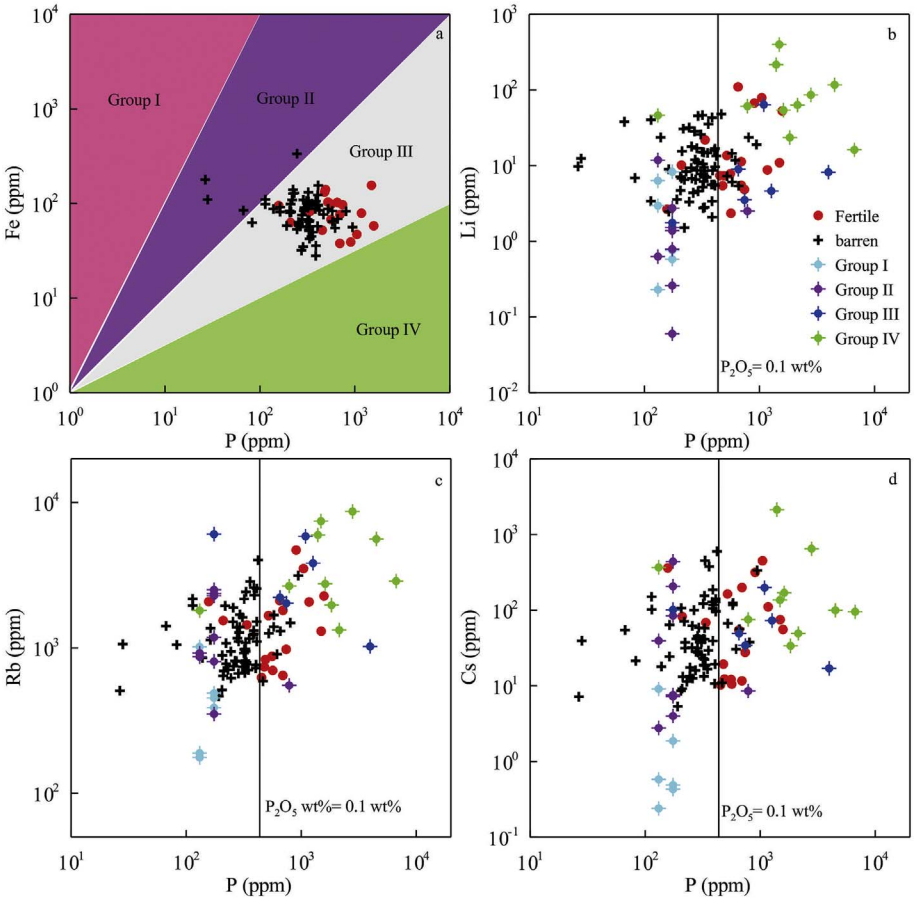

Fig. 6. a) the Fe vs. P discrimination plot of pegmatites. All data for the K-feldspar of the mineralized pegmatites (red circle) and almost all data for the K-feldspars of the barren pegmatites (black cross) are plotted in the Group III field. The fields are based on Sánchez-Muñoz et al. (2017); b) Li vs. P for K-feldspars from pegmatite; c) Rb vs. P for K-feldspars from pegmatite; d) Cs vs. P for K-feldspars from pegmatites. The data from Group I to Group IV are from Sánchez-Muñoz et al. (2017). (For interpretation of the references to color in this figure legend, the reader is referred to the web version of this article.)

with the P_2O_5 content and the K-feldspar species (Sánchez-Muñoz et al., 2012). According to London (1992), alkali feldspar, rather than phosphate minerals, is the major host of P_2O_5 in Ca-poor peraluminous magmatic system. Since then, phosphorus-rich K-feldspars have been identified in many granite rocks and pegmatite veins (e.g., Frýda and Breiter, 1995; Kontak et al., 1996; Breiter, 1997).

London et al. (1993) calibrated the partition coefficient for phosphorus between Ca-free alkali feldspars and melt as a function of the ASI (Aluminum Saturation Index) ($D_P^{Afs/melt} = 2.05^*ASI - 1.75$). Although bulk composition analysis of pegmatites is hampered by the exceptionally coarse grain-size and textural heterogeneity, the melt ASI can be estimated using the occurrence of peraluminous minerals. The typical peraluminous mineral in studied pegmatites is tourmaline. According to the experimental results, the ASI of granitic melt coexisting with tourmaline is approximately 1.2–1.3 when the crystallization temperature is between 650 and 750 °C (Acosta-Vigil et al., 2003). The calculated partition coefficient is about 0.8–1.0, so the high P_2O_5 content of alkali feldspars indicates high concentrations of this element in the melt from which the pegmatites crystallized.

Aside from the mineralized pegmatite from Keketuohai district, P-rich K-feldspars were reported in other rare-element mineralized pegmatites from Chinese Altay and other pegmatite district around the world. The pegmatites with P-rich K-feldspars from other pegmatite district were shown. The K-feldspars of the rare-element pegmatites, such as Halata, Qiukuer, and Jiamukai from the Altay orogen, Dan Patch, Bull Moose, Helen Beryl, Tip Top, and Tin Mountain from Black Hills, South Dakota, Tanco from Manitoba, Věžná from the Czech Republic, Varuträsk and Utö from Sweden and Luolamäki and Viitaniemi from Finland, usually contain P-rich K-feldspar (London et al., 1990; Tang et al., 2013). The K-feldspar from group III and goup IV pegmatites reported by Sánchez-Muñoz et al. (2012) also exhibited P-rich features.

From the above, it implies that the high contents of mineralized elements (Li, Rb and Cs), and phosphorus in K-feldspar from rare-element mineralized pegmatites reflect the high content of these elements in the initial magmatic and/or evolved magmatic melt. Undoubtedly, the pegmatite with the greatest economic potential for rare metal enrichment should contain K-feldspar with high Li, Rb and Cs. However, in many cases, Li, Rb, and Cs are easily released during the subsolidus transformation processes (Si-Al ordering, transformation twinning and recrystallization twinning, as described in Sánchez-Muñoz et al., 2012).

Novák et al. (1996) inferred that phosphorus would be remobilized by the muscovitization of P-rich feldspars in late- and postmagmatic stages of granite evolution. This process can be experessed by the reaction: K-rich Kfs + zinnwaldite = P-poor Kfs + muscovite + Fe-phosphate. However, Breiter et al. (2002) observed that phosphorus was liberated preferentially from albites, while its content in Kfs decreased only insignificantly during hydrothermal alteration process. Sánchez-Muñoz et al. (2017) also found P are much more firmly held in the structure than Li, Rb, and Cs do during the transformation and alteration process. Therefore, P_2O_5 always keeps its pristine character, and using P_2O_5 contents of Kfs are promising method for discriminating different types of pegmatites.

Our data and previous studies show that the P_2O_5 content of K-feldspar is more effective than the content of Li, Rb and Cs, in evaluating the Be, Nb and Ta mineralization potential of a pegmatite and therefore act as a good indicator for prospecting pegmatite-type rare-metal ore deposits in Altay, NW China.

6. Implications for ore prospecting in the Chinese Altay

The model that states that pegmatites are products of crystallization

from residual granitic melt is widely accepted. According to this model, pegmatites should be distributed around the parental granite. Therefore identification of fertile parental granite is an important exploration tool in the search for rare-metal pegmatites, because their discovery can greatly reduce the required search area (Selway et al., 2005; Trueman and Černý, 1982). More than 100,000 granitic pegmatite veins are exposed in the Chinese Altay orogen and these pegmatites predominately belong to the LCT family. Recent research has shown that these pegmatites were mainly emplaced between Late Permian and Triassic (Liu et al., 2014; Lv et al., 2012; Ma, 2014; Ren et al., 2011; Wang et al., 2007; Zhang et al., 2016; Zhou et al., 2015). However, just three Mesozoic plutons are identified in the Chinese Altay orogen: Ala'er I-type granite (ca. 220 Ma), Shangkelan I-type granite (ca. 203 Ma), and Jiangjunshan A-type granite (ca. 151 Ma) (Wang et al., 2014). Therefore, the parental granites of the pegmatites in Chinese Altay may still remain hidden. Because of the high altitude, dry climate, and lack of soil in Chinese Altay, it is also hard to use techniques such as stream-sediment geochemistry, till sampling and float-chasing, which can be utilized in other pegmatite districts (Trueman and Černý, 1982).

The emplacement of the rare-element pegmatite is usually accompanied by alterations in the host-rock and the development of an alkali-enriched exomorphic aureole surrounding the host rock. Bulk whole-rock analysis of metasomatically altered host rock may be a useful exploration tool for finding rare-metal pegmatites. However, the thickness of the alteration aureole can be variable and is constrained by both of features and compositions of the wall rock and the pegmatite. In Chinese Altay, the host rocks for pegmatites are mainly Paleozoic metasediments and igneous rocks (amphibolite or granite). However, the alteration aureole is very thin, which makes it difficult to take aureole samples and use it to evaluate potential resources in the pegmatite.

The identification of a zonal distribution of different pegmatite types in individual pegmatite groups, districts, or field is one of the most important aspects of pegmatite exploration. It narrows the search area for specific types of mineralization on the surface, and its establishment constitutes the first step towards developing a three-dimensional model of pegmatite distribution, which assists in a search for hidden deposits (Trueman and Černý, 1982). However, this is difficult because the pegmatite population in Chinese appears homogeneous. In the past sixty to seventy years, nor regional zonation of pegmatites in Chinese Altay has been identified.

Favorably, pegmatites in Chinese Altay are easily found because they are well exposed. Once the pegmatite is located, the next step is to quickly evaluate its mineralization potential based on some geochemical indicators. These methods are a cost-saving procedure which should precede any drilling.

The above analysis shows that the determination of the phosphorus in K-feldspar from the early-formed textural zones of pegmatite is a good method for indicating potential rare metals resources in pegmatite districts. According to the results reported above, rare metal-mineralized LCT type pegmatite is characterized by k-feldspar with high content of phosphorus, and thus, > 0.1 wt% P_2O_5 in k-feldspar can act as a good indicator for prospecting LCT pegmatite-type rare-metal ore deposits in Chinese Altay.

Acknowledgement

This work was financially supported by National Natural Science Foundation of China (Grant No. 41372104 and 41372104) and Research Project of Xinjiang Nonferrous Metals Industry (Group) Co., Ltd. (Grant No. YSKY2011-02).

Appendix A. Supplementary data

Supplementary data associated with this article can be found in the online version, at doi: https://doi.org/10.1016/j.gexplo.2017.11.015. These data include the Google map of the most important areas described in this article.

References

Acosta-Vigil, A., London, D., Morgan, G., Dewers, T., 2003. Solubility of excess alumina in hydrous granitic melts in equilibrium with peraluminous minerals at 700–800 °C and 200 MPa, and applications of the aluminum saturation index. Contrib. Mineral. Petrol. 146, 100–119.

Alfonso, P., Melgarejo, J.C., Yusta, I., Velasco, F., 2003. Geochemistry of feldspars and muscovite in granitic pegmatite from Cap De Creus field, Catalonia, Spain. Can. Mineral. 41, 103–116.

Breiter, K., 1997. Mineralogical evidence for two magmatic stages in the evolution of an extremely fractionated P-rich rare-metal granite: the Podlesi stock, Krusne Hory, Czech Republic. J. Petrol. 38, 1723–1739.

Breiter, K., Frýda, J., Leichmann, J., 2002. Phosphorus and rubidium in alkali feldspars: case studies and possible genetic interpretation. Bulletin of the Czech Geological Survey 77, 93–104.

Cai, K., Sun, M., Yuan, C., Zhao, G., Xiao, W., Long, X., Wu, F., 2011a. Geochronology, petrogenesis and tectonic significance of peraluminous granites from the Chinese Altai, NW China. Lithos 127, 261–281.

Cai, K., Sun, M., Yuan, C., Zhao, G., Xiao, W., Long, X., Wu, F., 2011b. Prolonged magmatism, juvenile nature and tectonic evolution of the Chinese Altai, NW China: evidence from zircon U–Pb and Hf isotopic study of Paleozoic granitoids. J. Asian Earth Sci. 42, 949–968.

Cai, K., Sun, M., Yuan, C., Zhao, G., Xiao, W., Long, X., 2012. Keketuohai mafic–ultramafic complex in the Chinese Altai, NW China: petrogenesis and geodynamic significance. Chem. Geol. 294–295, 26–41.

Černý, P., Ercit, T.S., 2005. The classification of granitic pegmatites revisited. Can. Mineral. 43, 2005–2026.

Černý, P., Smith, J.V., Mason, R.A., Delaney, J.S., 1984. Geochemistry and petrology of feldspar crystallization in the Vezna pegmatite, Czechoslovakia. Can. Mineral. 22, 631–651.

Černý, P., Meintzer, R.E., Anderson, A.J., 1985. Extreme fractionation in rare-element granitic pegmatites; selected examples of data and mechanisms. Can. Mineral. 23, 381–421.

Frýda, J., Breiter, K., 1995. Alkali feldspars as a main phosphorus reservoirs in rare-metal granites: three examples from the Bohemian Massif (Czech Republic). Terra Nova 7, 315–320.

Gordiyenko, V.V., 1971. Concentrations of Li, Rb, and Cs in potash feldspar and muscovite as criteria for assessing the rare-metal mineralization in granite pegmatites. Int. Geol. Rev. 13, 134–142.

Kontak, D.J., Martin, R.F., Richard, L., 1996. Patterns of phosphorus enrichment in alkali feldspar, South Mountain Batholith. Nova Scotia, Canada. Eur. J. Mineral. 8, 805–824.

Linnen, R.L., Van Lichtervelde, M., Černý, P., 2012. Granitic pegmatites as sources of strategic metals. Elements 8, 275–280.

Liu, Y., Hu, Z., Gao, S., Günther, D., Xu, J., Gao, C., Chen, H., 2008. In situ analysis of major and trace elements of anhydrous minerals by LA-ICP-MS without applying an internal standard. Chem. Geol. 257, 34–43.

Liu, F., Zhang, Z.-X., Li, Q., Zhang, C., Li, C., 2014. New precise timing constraint for the Keketuohai No. 3 pegmatite in Xinjiang, China, and identification of its parental pluton. Ore Geol. Rev. 56, 209–219.

London, D., 1992. Phosphorus in S-typ magmas: the P_2O_5 content of feldspars from peraluminous granites, pegmatites, and rhyolites. Am. Mineral. 77, 126–145.

London, D., 2008. Pegmatites. Mineralogical Association of Canada.

London, D., Černý, P., Loomis, J.L., Pan, J.J., 1990. Phosphorus in alkali feldspars of rare-element granitic pegmatites. Can. Mineral. 28, 771–786.

London, D., Morgan, G.B., Babb, H.A., Loomis, J.L., 1993. Behavior and effects of phosphorus in the system Na_2O-K_2O-Al_2O_3-SiO_2-P_2O_5-H_2O at 200 MPa(H2O). Contrib. Mineral. Petrol. 113, 450–465.

Lv, Z.-H., Zhang, H., Tang, Y., Guan, S.-J., 2012. Petrogenesis and magmatic–hydrothermal evolution time limitation of Kelumute No. 112 pegmatite in Altay, Northwestern China: evidence from zircon UPb and Hf isotopes. Lithos 154, 374–391.

Ma, Z.-L., 2014. Zircon U-Pb Dating and Hf Isotopes of Pegmatites from the Kaluan Mining Area in Altay, Xinjiang and Their Genetic Relationship with Halong Granite. Graduate University of Chinese Academy of Sciences, Beijing.

Neiva, A.M.R., 1995. Distribution of trace elements in feldspars of granitic aplites and pegmatites from Alijó-Sanfins, Northern Portugal. Mineral. Mag. 59, 35.

Novák, J.K., Pivec, E., Štemprok, M., 1996. Hydrated iron phosphates in muscovite-albite granite from Waidhaus (Oberpfalz, Germany). J. Czech Geol. Soc. 41, 201–207.

Oyarzábal, J., Galliski, M.Á., Perino, E., 2009. Geochemistry of K-feldspar and muscovite in rare-element pegmatites and granites from the totoral pegmatite field, San Luis, Argentina. Resour. Geol. 59, 315–329.

Ren, B.-Q., Zhang, H., Tang, Y., Lv, Z.-H., 2011. LA-ICP-MS U-Pb zircon geochronology of the Altai pegmatites and its geological significance. Acta Mineral. Sin. 31, 587–596 (in Chinese with English abstract).

Sánchez-Muñoz, L., García-Guinea, J., Zagorsky, V.Y., Juwono, T., Modreski, P.J., Cremades, A., Van Tendeloo, G., de Moura, O.J.M., 2012. The evolution of twin patterns in perthitic K-feldspar from granitic pegmatites. Can. Mineral. 50, 989–1024.

Sánchez-Muñoz, L., Müller, A., Andrés, S.L., Martin, R.F., Modreski, P.J., de Moura, O.J.M., 2017. The P-Fe diagram for K-feldspars: a preliminary approach in the discrimination of pegmatites. Lithos 272–273, 116–127.

Selway, J.B., Breaks, F.W., Tindle, A.G., 2005. A review of rare-element (Li-Cs-Ta) pegmatite exploration techniques for the Superior Province, Canada, and large worldwide tantalum deposits. Explor. Min. Geol. 14, 1–30.

Sengör, A., Natal'In, B., Burtman, V., 1993. Evolution of the Altaid tectonic collage and Palaeozoic crustal growth in Eurasia. Nature 364, 22.
Shearer, C.K., Papike, J.J., Laul, J.C., 1985. Chemistry of potassium feldspars from three zoned pegmatites, Black Hills, South Dakota: implications concerning pegmatite evolution. Geochim. Cosmochim. Acta 49, 663–673.
Simpson, D.R., 1977. Aluminum phosphate variants of feldspar. Am. Mineral. 62, 351–355.
Smeds, S.A., 1992. Trace elements in potassium-feldspar and muscovite as a guide in the prospecting for lithium- and tin-bearing pegmatites in Sweden. J. Geochem. Explor. 42, 351–369.
Tang, Y., Zhang, H., 2015. Lanthanide tetrads in normalized rare element patterns of zircon from the Koktokay No. 3 granitic pegmatite, Altay, NW China. Am. Mineral. 100, 2630–2636.
Tang, Y., Zhang, H., Su, G.-Z., 2013. Phosphorus in alkali feldspars as an indicator for prospecting for pegmatite-type rare-metal ore deposits in Altay, NW China. Geochem.: Explor., Environ., Anal. 13, 3–10.
Taylor, W.H., 1965. The Feldspars. In: Bragg, W.L., Claringbull, G.F. (Eds.), Crystal Structure of Minerals. Bell and Sons, London.
Tian, Y., Qin, K.Z., Zhou, Q.F., Paterson, G., 2016. Structural control on the shape of intrusions in the Koktokay ore district, Chinese Altai, north western China. J. Struct. Geol. 83, 85–102.
Tong, Y., Wang, T., Jahn, B.-m., Sun, M., Hong, D.-W., Gao, J.-F., 2014. Post-accretionary permian granitoids in the Chinese Altai orogen: geochronology, petrogenesis and tectonic implications. Am. J. Sci. 314, 80–109.
Trueman, D., Černý, P., 1982. Exploration for rare-element granitic pegmatites. In: Granitic Pegmatites in Science and Industry. Vol. 8. Mineralogical Association of Canada, pp. 463–493 Short Course Handbook.
Wang, T., Hong, D.-W., Jahn, B.-M., Tong, Y., Wang, Y.-B., Han, B.-F., Wang, X.-X., 2006. Timing, petrogenesis, and setting of paleozoic synorogenic intrusions from the Altai Mountains, Northwest China: implications for the tectonic evolution of an accretionary orogen. J. Geol. 114, 735–751.
Wang, T., Tong, Y., Jahn, B.-M., Zou, T.-R., Wang, Y.-B., Hong, D.-W., Han, B.-F., 2007. SHRIMP U-Pb zircon geochronology of the Altai no. 3 pegmatite, NW China, and its implications for the origin and tectonic setting of the pegmatite. Ore Geol. Rev. 32, 325–336.
Wang, T., Tong, Y., Li, S., Zhang, J.-J., Shi, X.-J., Li, J.-Y., Han, B.-F., Hong, D.-W., 2010. Spatial and temporal variation of granitoids in the Altay orogen and their implications for tectonic setting and crustal growth: perspectives from Chinese Altay. Acta Petrol. Mineral. 29, 595–618 (in Chinese with English abstract).
Wang, T., Jahn, B.-m., Kovach, V.P., Tong, Y., Wilde, S.A., Hong, D.-w., Li, S., Salnikova, E.B., 2014. Mesozoic intraplate granitic magmatism in the Altai accretionary orogen, NW China: implications for the orogenic architecture and crustal growth. Am. J. Sci. 314, 1–42.
Windley, B.F., Alfred Kröner, A., Guo, J.-H., Qu, G.-S., Li, Y.-Y., Zhang, C., 2002. Neoproterozoic to Paleozoic geology of the Altai Orogen, NW China: new zircon age data and tectonic evolution. J. Geol. 110, 719–737.
Yu, Y., Sun, M., Long, X., Li, P., Zhao, G., Kröner, A., Broussolle, A., Yang, J., 2017. Whole-rock Nd–Hf isotopic study of I-type and peraluminous granitic rocks from the Chinese Altai: constraints on the nature of the lower crust and tectonic setting. Gondwana Res. 47, 131–141.
Yuan, C., Sun, M., Long, X.-P., Xia, X.-P., Xiao, W.-J., Li, X.-H., Lin, S.-F., Cai, K.-D., 2007a. Constraining the deposition time and tectonic background of the Habahe Group of the Altai. Acta Petrol. Sin. 23, 1635–1644.
Yuan, C., Sun, M., Xiao, W., Li, X., Chen, H., Lin, S., Xia, X., Long, X., 2007b. Accretionary orogenesis of the Chinese Altai: insights from Paleozoic granitoids. Chem. Geol. 242, 22–39.
Zhang, A.C., Wang, R.C., Jiang, S.Y., Hu, H., Zhang, H., 2008. Chemical and textural features of tourmaline from the spodumene-subtype Koktokay No. 3 pegmatite, Altai, northwestern China: a record of magmatic to hydrothermal evolution. Can. Mineral. 46, 41–58.
Zhang, Y.-F., Lin, X.-W., Guo, Q.-M., Wang, X., Zhao, D.-C., Dang, C., Yao, S., 2015. LA-ICP-MS zircon U-Pb dating and geochemistry of Aral Granitic Plutons in Koktokay Area in the Southern Altay Margin and their source significace. Acta Geol. Sin. 89, 339–354 (In Chinese with English abstract).
Zhang, X., Zhang, H., Ma, Z.-L., Tang, Y., Lv, Z.-H., Zhao, J.-Y., Liu, Y.-L., 2016. A new model for the granite–pegmatite genetic relationships in the Kaluan–Azubai–Qiongkuer pegmatite-related ore fields, the Chinese Altay. J. Asian Earth Sci. 124, 139–155.
Zhang, C., Liu, L., Santosh, M., Luo, Q., Zhang, X., 2017. Sediment recycling and crustal growth in the Central Asian Orogenic Belt: evidence from Sr–Nd–Hf isotopes and trace elements in granitoids of the Chinese Altay. Gondwana Res. 47, 142–160.
Zhou, Q., Qin, K., Tang, D., Tian, Y., Cao, M., Wang, C., 2015. Formation age and evolution time span of the Koktokay No. 3 Pegmatite, Altai, NW China: evidence from U-Pb Zircon and ^{40}Ar-^{39}Ar Muscovite Ages. Resour. Geol. 65, 210–231.
Zou, T., Li, Q., 2006. Rare and Rare Earth Metallic Deposits in Xinjiang, China. Geological Publishing House, Beijing (in Chinese).
Zou, T., Zhang, X., Jia, F., Wang, R., Cao, H., Wu, P., 1986. A discussion about contributing factor of the Altai No. 3 pegmatite. Mineral Deposits 5, 34–48 (in Chinese with English abstract).
Zou, T.-R., Chao, H.-Z., Wu, B.-Q., 1989. Orogenic and anorogenic granitoids of Altay Mountains of Xinjiang and their discrimination criteria. Acta Geol. Sin. 2, 45–64.